

Chapter-II

Theoretical Details

This chapter gives the general introduction of transition metal oxide glasses, small polaron and mixed conducting system. Different models for ac and dc conductivity is also discussed. At the end, theoretical background of various techniques used for characterization is also included.

Most of the glasses are insulating in nature but the addition of transition metal oxides (TMO) such as V_2O_5 , Fe_2O_3 etc. makes these glasses semiconducting in nature. These glasses have attracted scientific interest and technical applications. Systems based on glass forming compounds usually offer the possibility of preparing the solids within a much wider range of composition than their crystalline analogs. The differences in composition can result in considerable differences in the physical properties e.g., the electrical conductivity of the glasses. Therefore, silver oxide containing barium vanado-tellurite glasses have been chosen for the present study, which shows mixed conducting nature.

2.1 Transition Metal Oxide Glasses:

Glasses which have the major constituent as oxides of transition metal such as V_2O_5 , Fe_2O_3 , MoO_3 etc. are known as transition metal oxide glasses. These glasses are of the charge-charge transfer or mixed valence type of semiconducting conductor. These glasses exhibit semiconducting behavior due to the presence of multivalent states of transition metal ions in the glassy matrices [1, 2] (e.g., V^{+4} and V^{+5} in vanadate and Cu^{+1} and Cu^{+2} in cuprate glasses). It is generally agreed that the dc electrical conduction in these glassy semiconductors take place by the hopping movement of small polarons between different valence states of TMI sites [1, 2, 3-7]. Consequently, the conduction is through the d-levels of the transition metal and as the d-overlap is small, the bandwidth is also small, the effective mass m^* is large and the electron wavelength $\lambda = \frac{h}{(2\pi m^* kT)^{1/3}}$ is of the order of lattice spacing. The electron is, therefore, essentially localized and almost certainly self trapped through the formation of small polaron conduction occurred

by hopping but localization due to disorder makes a contribution to conduction too. Austin and Mott [2] described a conduction mechanism in non-crystalline solids. Anderson et. al. [8] had given a clear picture about localization of electron and Miller & Abraham [9] gave a mechanism of conductivity in Si and Ge. An electron in non-crystalline solids moves by thermally activated hopping from one localized state to another one and activation energy associated with this hopping, due to localization of its state, is quantized energy for a certain range. An exchange of energy with phonon causes the localization in these glasses.

2.2 Small polaron conduction:

A polaron is a conceptual construct consisting of an electron which occupies each site in its motion through the crystal for a time sufficiently long that the ions, of which the crystal is composed, have time to relax into a configuration appropriate to the altered charge on the host ion. This alteration is largest in the neighborhood of the host ion. The electron and its accompanying distortion may be treated as a single particle called the '*polaron*' [2, 10]. The nature of the polaron transport mechanism in the lattice depends upon the integral of the overlap of the electron wave function on adjacent sites. The polaron binding energy is that change in the electron potential energy that comes about as a result of the lattice distortion that the electron induces in the neighborhood of its host. The size of the polaron (measured by the size of the induced lattice distortion) depends upon whether the electron overlap is larger or smaller than the binding energy of the polaron. If the overlap integral is small compared to the binding energy of the polaron, the linear dimensions of the polaron become comparable to the lattice spacing which is the

case of the *small polaron*. Now, it is obvious that we can attain the small polaron condition in two types of materials. Those materials in which the coupling of the electron to the lattice is particularly large producing a small ratio of overlap integral to polaron binding energy and also those materials in which a small value of the overlap (due to larger ion spacing etc.) yields a similar ratio of overlap to binding energy, should both show small polaron effects for appropriate concentrations of ions. That is, the small polaron describes both the case of “*strong electron-lattice interactions*” and that of strongly “*localized electrons*”.

2.3 Mixed Conducting System:

Electrical properties of oxide glasses containing large amounts of transition metal ions are determined by their presence in two different valence states. Electrical conduction in these semiconducting glasses is explained on the theories of Mott and Austin [2]. Many workers [2, 8-12] had reported on such type of materials and suggested the carrier mechanism in such materials be due to small polaron. When an alkali oxide is added during glass preparation, one may also expect mobile alkali ions to contribute to the charge transport and the mixed conductivity to be observed. The dc ionic conduction in glasses occurs by the migration of cations between occupied and vacant sites that are randomly distributed in the glass structure.

According to Frenkel et. al. [13], the ions causing conduction leave their positions and enter interstitial sites, and thus become quasi-free ions with the ability to migrate. At the same time, their former positions are free, so that vacancy conduction becomes possible. Generally, ionic conductivity depends on alkali

concentration and ion mobility. Assuming that the motion of alkali ions and polarons are independent, we may expect electrical conductivity to increase with increasing alkali content.

It is known that in the systems $\text{Li}_2\text{O}-\text{WO}_3-\text{P}_2\text{O}_5$ [14] and $\text{Na}_2\text{O}-\text{V}_2\text{O}_5-\text{TeO}_2$ [15], by modifying the composition it is possible to prepare glasses with predominantly ionic or electronic conduction. Other studies [16, 17] also showed that the same holds for silver-vanadate phosphate glasses of the quaternary system $\text{AgI}-\text{Ag}_2\text{O}-\text{V}_2\text{O}_5-\text{P}_2\text{O}_5$. Ternary systems $\text{AgI}-\text{Ag}_2\text{O}-\text{P}_2\text{O}_5$ and $\text{AgI}-\text{Ag}_2\text{O}-\text{V}_2\text{O}_5$ with a low concentration of V_2O_5 are well known as super ionic glasses [18, 19]. On the other hand, binary glasses $\text{V}_2\text{O}_5-\text{P}_2\text{O}_5$ of high V_2O_5 content exhibit electronic (polaronic) conductivity [20, 21].

Our aim is to study the electrical properties of the glasses of the quaternary system $\text{BaO}-\text{Ag}_2\text{O}-\text{V}_2\text{O}_5-\text{TeO}_2$ exhibiting mixed ionic-electronic conduction. In this system V_2O_5 is the main glass former and the matrix for electronic conduction, TeO_2 is also a supporting glass former, whereas Ag_2O and BaO are the glass modifiers.

2.4 Models for DC Conductivity:

2.4.1 Mott's Model for DC Conductivity:

Mott has investigated the conduction model for glasses containing transition metal ions. Conduction in these glasses is considered in terms of phonon assisted hopping of small polaron between localized states. According to Mott's model, if a carrier remains for a sufficiently long time on a particular atomic or ionic site (i.e., V^{+5}) than the period of vibration, then the ions in the neighborhood of this

excess charge will get enough time to get a new equilibrium position consistent with the presence of this additional charge. This will generate potential well for additional carriers. A carrier may bound to a state due to a deep potential well. Thus, a bound carrier and its induced lattice deformation in a solid, is termed as a "Polaron". A Polaron is said to be small if a potential well is localized at a single atomic or ionic site. Fig.(2.1) shows a clear picture of this model.

As shown in Fig 2.1 (a), initially an electron is trapped in a potential well and the smallest activation energy corresponds to this state is given in Fig 2.1 (b), when thermal fluctuation ensures that the wells have the same depths. The energy required for this configuration is given by

$$W_H = \frac{1}{2}W_P = \frac{e^2}{4\epsilon_p r_p} \dots\dots\dots(2.1)$$

where $\epsilon_p = \left[\left(\frac{1}{\epsilon_\infty} \right) - \left(\frac{1}{\epsilon_s} \right) \right]^{-1}$, ϵ_s and ϵ_∞ are the static and high frequency dielectric constants of this material. Electron hopping process is between a and b ions when the states are localized, r_p is the polaron radius i.e., a distance from the electron beyond which the medium is polarized, W_H is the activation energy and W_P is the small polaron binding energy defined as the total potential energy of the electron and that of its attendant lattice distortion.

At a large distance from the electron, the potential energy of another electron in a crystal is $e^2/\epsilon_s r$, whereas if the ions could not move, it would be $e^2/\epsilon_\infty r$, where ϵ_s and ϵ_∞ are the static and high frequency dielectric constants.

Thus the potential energy $V_p(r)$ in the potential well due to the displacement of the ions is given by

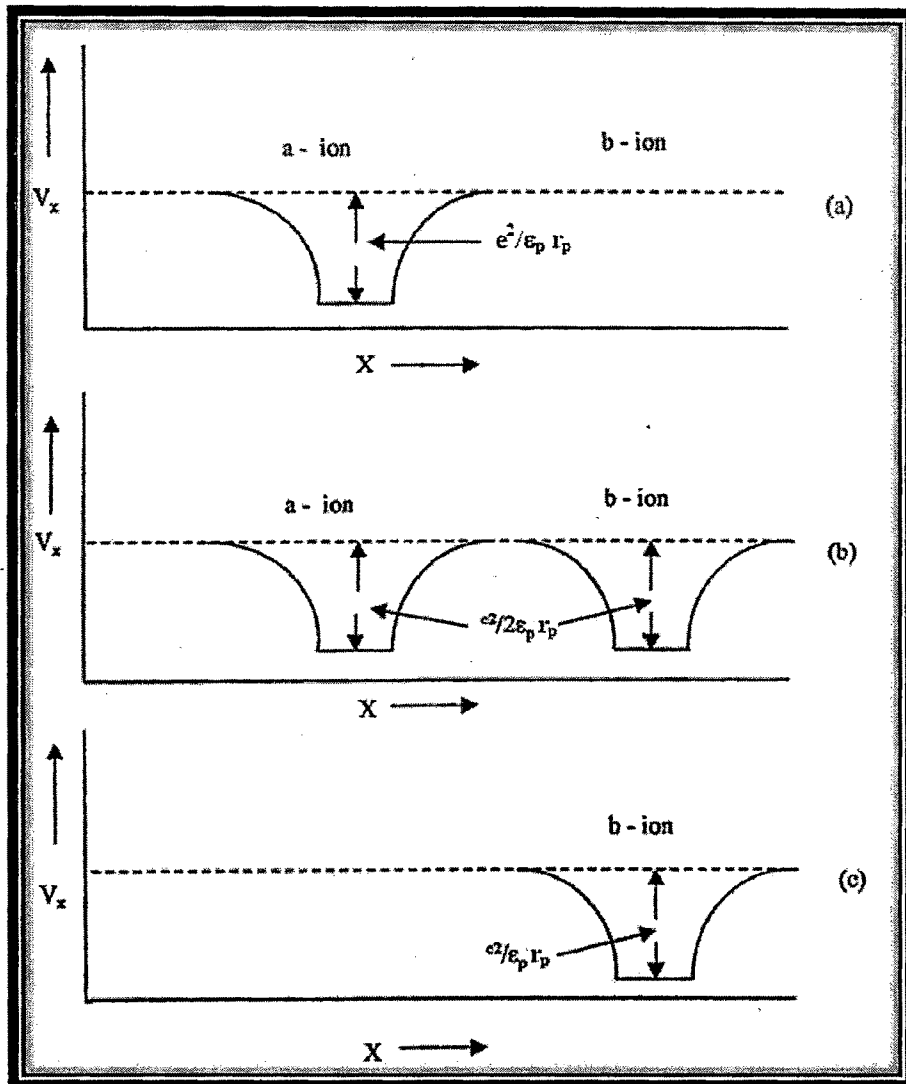


Fig.2.1: Picture of small Polaron Conduction Model: The polarization wells for two transition metal ions in glass during hopping process: (a) before hopping (b) thermally activated states when electron can move (c) after hopping.

$$V_p(r) = -\frac{e^2}{(\epsilon_p r)} \quad \dots\dots\dots (2.12)$$

where ϵ_p is the effective dielectric constant and r is the radius of an ion.

The electron digs a potential well for itself for which

$$V_p(r) = -\frac{e^2}{\epsilon_p r} \quad \text{for } r > r_p \quad \dots\dots (2.13)$$

$$= -\frac{e^2}{\epsilon_p r_p} \quad \text{for } r < r_p \quad \text{-----}(2.14)$$

The value of r_p can be determined by minimizing the kinetic energy of electron i.e., by localized state.

In Mott's model, conductivity for the nearest neighbor hopping in the high temperature region ($T > \theta_{D/2}$) (θ_D is the Debye temperature) is given by

$$\sigma = \nu_0 \left[\frac{Ne^2 R^2 c(1-c)}{kT} \right] \exp(-2\alpha R) \exp\left(\frac{-W}{kT}\right) \quad \dots\dots\dots (2.15)$$

where ν_0 is the optical phonon frequency (generally $\nu_0 \sim 10^{13}$), N is the transition metal ion sites per unit volume, C is the ratio of concentration of ions in

low valance state to the total concentration of ion i.e., $\frac{V^{-4}}{V_{total}}$, α is the electron

wave function decay constant, W is the activation energy for dc conduction and

R is the average site separation.

Assuming a strong electron-phonon interaction, Austin & Mott, have shown that [2, 22].

$$W = W_H + \frac{1}{2}W_D \quad \left(\text{for } T > \frac{\theta_D}{2}\right) \text{ In non-adiabatic region. } \dots\dots\dots(2.16)$$

$$W = W_D \quad \left(\text{for } T > \frac{\theta_D}{4}\right) \text{ In adiabatic region.} \quad \dots\dots\dots(2.17)$$

where T is the absolute temperature, θ_D is the Debye temperature defined by $\hbar\nu_0 = k\theta_D$ (\hbar is the Planck's constant, ν_0 is the optical phonon frequency, k is the Boltzmann constant) and $W_H \approx \frac{1}{2}W_p$, where W_p is the polaron binding energy and W_H is the polaron hopping energy. Equation (2.15) is for the hopping of polarons in non-adiabatic region. For the hopping of polarons in the adiabatic region, the tunneling term reduces to unity i.e., $\exp(-2\alpha R) \rightarrow 1$.

Then equation (2.15) becomes,

$$\sigma = \sigma_0 \exp\left(\frac{-W}{kT}\right) \quad \text{-----} (2.18)$$

where $\sigma_0 = \left(\frac{\nu_0 e^2 c(1-c)}{kTR}\right)$ is the pre exponential term for conductivity and can be estimated from the conductivity data.

Mott [23] has pointed out that at very low temperatures, the observed values of W_D (disorder energy) should approach zero because the most probable jump will not be to nearest neighbors but to more distant sites where the energy difference is small. The conductivity for variable range hopping is given by the following Equation

$$\sigma = A \exp\left(\frac{-B}{T^{1/4}}\right) \quad \dots\dots\dots(2.19)$$

where A and B are constants and given by

$$A = \left[\frac{e^2}{2(8\pi)^{1/2}}\right] \nu_0 \left[\frac{N(E_f)}{\alpha kT}\right]^{1/2} \quad \dots\dots\dots(2.20)$$

and
$$B = 2.1 \left[\frac{\alpha^3}{kN(E_f)} \right]^{1/4} \dots\dots\dots(2.21)$$

where $N(E_f)$ is the density of states at the Fermi level, α describes the decay of the localized state wave function and ν_0 is the optical phonon frequency ($\approx 10^{13} s^{-1}$) [24]. So, the variable range hopping model predicts a $T^{-1/4}$ dependence of the logarithm of conductivity at low temperatures. Similar temperature dependence of the conductivity at low temperatures has been also obtained by Ambegaokar and co-workers [25] on the basis of percolation model. Thus the equation for conductivity, in non-crystalline solids, carries a great importance and gives a clear picture of conduction in such types of materials.

2.4.1.1 Small polaron and large polaron hopping:

At a given density of electrons $N(e)$, the mobility of electrons is zero at a finite E, i.e., $\sigma_E(0)$ vanishes for these energies then the electron is said to be localized with energy E. If states are localized, mobility μ vanishes at T=0. At finite temperature, the mobility is essentially due to interaction with phonons. In principle, localization ($\sigma_E(0)=0$) can occur for a given energy E for the following reasons;

- i) a random potential at each atom [3],
- ii) fluctuations in the density or mean interatomic distance and
- iii) absence of long range order.

When a state is localized, we consider two approximations for hopping after determining small polaron radius (r_p). First is when the effective mass m^* of the

electron is too high and the kinetic energy $\frac{\hbar^2 \pi^2}{m^* r_p^2}$ due to the localization of the wells is very small or negligible. Then r_p (polaron radius) must be less than the interatomic distance R i.e., ($r_p < R$) and the polaron is said to be "small polaron". In this case total potential energy of the electron becomes

$$-W_p = -\frac{1}{2} \left(\frac{e^2}{\epsilon_p r_p} \right) \dots\dots\dots(2.22)$$

Second is when the polaron radius r_p is greater than the interatomic distance R i.e., ($r_p > R$), then the polaron hopping becomes a "large polaron" due to smaller

m^* . Here we have to add the kinetic energy $\frac{\hbar^2 \pi^2}{2m^* r_p^2}$ of an electron so in this case

total energy is given by

$$-W_p = -\frac{1}{2} \frac{e^2}{\epsilon_p r_p} + \frac{\hbar^2 \pi^2}{2m^* r_p^2} \dots\dots\dots(2.23)$$

Eq.2.23 will be minimum when

$$r_p = \frac{2\pi^2 \hbar^2 \epsilon_p}{m^* e^2} \dots\dots\dots(2.24)$$

Eq.2.1 is corrected for larger value of R i.e., distance between the centers.

Therefore, for a larger value of R , two polarization clouds overlap and W_H

becomes dependent on jumping distance R . Mott in 1968 [1] modified Eq.2.1 as

$$W_H = \frac{1}{4} \left(\frac{e^2}{\epsilon_p} \right) \left(\frac{1}{r_p} - \frac{1}{R} \right) \dots\dots\dots(2.25)$$

where ϵ_p is the effective dielectric constant, r_p is the small polaron radius and

R is the average site separation calculated by the relation

$$R = \left(\frac{1}{N}\right)^{1/3} \dots\dots\dots(2.26)$$

Polaron radius for a crystalline material is given by

$$r_p = \frac{1}{2} \left(\frac{\pi}{6N}\right)^{1/3} = \left(\frac{\pi}{6}\right)^{1/3} \left(\frac{R}{2}\right) \dots\dots\dots(2.27)$$

where N is the number of sites (i.e., V_{total} ions in V_2O_5) per unit volume [26] and can be calculated as

$$N = 2 \left[\left(\frac{F_w}{M_w} d \right) N_A \right] \dots\dots\dots(2.28)$$

where d is the density of the glass sample, F_w is the weight fraction of V_2O_5 , M_w is the molecular weight of V_2O_5 and N_A is the Avogadro number, respectively.

2.4.1.2 Nature of polaron hopping:

In non crystalline solids having a disordered system, an additional term W_D (disorder energy) i.e., energy difference arising from the differences of neighbors between a and b sites (Fig. 2.1), may appear in the activation energy for the hopping process. In this case, the total activation energy for the hopping process in the high temperature region is [2]

$$W = W_H + \frac{1}{2} W_D + \frac{W_D^2}{16W_H} \dots\dots\dots(2.29)$$

or
$$W = \frac{(W_D + 4W_H)^2}{16W_H} \dots\dots\dots(2.30)$$

If $W_D < W_H$

$$W \approx W_H + \frac{1}{2}W_D \quad \dots\dots\dots(2.31)$$

For a disordered lattice, the coincidence of electronic energy level of the bound electron sites with the local electronic energy level on neighborhood gives rise to transfer of a small polaron. This transfer probability is given by,

P = probability of coincidence \times (probability of transfer when coincidence occurs)

$$= \left(\frac{\omega_0}{2\pi} \right) \exp\left(\frac{-W}{kT} \right) \times P \quad \dots\dots\dots(2.32)$$

where P is probability of transfer when coincidence occurs, which is related to two types of cases. If the value of P (probability of transfer) is;

- i) equal to unity ($P = 1$) \rightarrow In this case time duration of coincident event is long compared with the time it takes an electron to transfer between two sites and electron always follows lattice motion.
- ii) less than unity ($P \ll 1$) \rightarrow When the time required for an electron to hop is large compared with the duration of a coincident event. In this case electron will not always follow lattice motion and miss many coincident events before making a hop.

In this case the probability of transfer P is given by [10]

$$P = \left(\frac{2\pi}{\hbar\omega_0} \right) \left[\frac{\pi}{4W_H kT} \right]^{1/2} J^2 \quad \dots\dots\dots(2.33)$$

where J is the electron transfer integral and is a measure of wave function overlap of the neighboring sites. If $J > \hbar\omega_0$ and the tunneling probability $\exp(-2\alpha R)$ is small, where α is a spatial decay constant of electron wave

function, then conduction is due to **adiabatic hopping**. A **non-adiabatic hopping** process would occur if $J < \hbar\omega_0$ (i.e., predominantly phonon energy). Hence P contains the factor $\exp(-2\alpha R)$.

In the frame work of Mott's model [1, 2, 3], the nature of hopping mechanism can be ascertained by a different method i.e., by plotting a graph between $\log \sigma$ and W at an arbitrary chosen temperature. If the estimated temperature calculated from the slope ($1/(2.303kT)$) of the plot, is close to T , it means $\exp(-2\alpha R)$ term of Eq. 2.15 does not contribute to the conductivity, then the adiabatic hopping process occurs in the glass system but if the estimated temperature is different from the chosen temperature, $\exp(-2\alpha R)$ term contributes to conductivity and non-adiabatic hopping occurs.

2.4.2 Molecular Crystal Model:

Holstein and co-workers [11, 27, 28] have investigated a generalized polaron hopping model assuming that the disorder energy, $W_D=0$, covering both the adiabatic and non-adiabatic hopping processes. Holstein has derived an expression for the dc conductivity in the non-adiabatic region as

$$\sigma = \left(\frac{3}{2}\right) \left(\frac{e^2 N R^2 J^2}{kT}\right) \left(\frac{\pi}{kT W_H}\right)^{1/2} \exp\left(\frac{-W_H}{kT}\right) \dots\dots\dots (2.34)$$

Conductivity in the adiabatic region is given by

$$\sigma = \left(\frac{8\pi}{3}\right) \left(\frac{e^2 N R^2 v_0}{kT}\right) \exp\left(\frac{-W_H - J}{kT}\right) \dots\dots\dots (2.35)$$

where N is the site concentration, J is the polaron band width related to the electron wave function overlap on adjacent sites.

According to this model, adiabatic and non-adiabatic condition may be separated depending on the value of J as below

$$\begin{aligned}
 J &> \left[\frac{2kTW_H}{\pi} \right]^{1/4} \left[\frac{h\nu_0}{\pi} \right]^{1/2} && \text{adiabatic hopping} \\
 &< \left[\frac{2kTW_H}{\pi} \right]^{1/4} \left[\frac{h\nu_0}{\pi} \right]^{1/2} && \text{non-adiabatic hopping}
 \end{aligned}
 \dots\dots\dots (2.36)$$

with the condition for the existence of a small polaron being $J \leq \frac{1}{3}W_H$. The polaron band width J can be estimated from [29, 23]

$$J \approx e^3 \frac{[N(E_f)]^{1/2}}{\epsilon_p^{3/2}} \dots\dots\dots (2.37)$$

The polaron band width J can also be estimated from the difference of mean value of hopping energy W_H and the experimental activation energy W i.e., by $J = W_{H(max)} - W$ [30]. By the estimation of the value of J , nature of hopping in several glasses was also reported [2, 22, 26, 29-36].

2.4.3 Schnakenberg's Model:

A more general polaron hopping model has been considered by Schnakenberg [37], where $W_D \neq 0$, in which optical multiphonon process determines the dc conductivity at high temperature, while at low temperatures, charge carrier transport is an acoustical one phonon-assisted hopping process. The temperature dependence of the dc conductivity in this model has the form

$$\sigma \approx T^{-1} \left[\sinh \left(\frac{h\nu_0}{2kT} \right) \right]^{1/2} \exp \left[- \left(\frac{4W_H}{h\nu_0} \right) \times \tanh \left(\frac{h\nu_0}{4kT} \right) \right] \exp \left(\frac{-W_D}{kT} \right) \dots (2.38)$$

The above equation predicts a temperature dependent hopping energy given by

$$W_H' = W_H \frac{\left[\tanh\left(\frac{hw_0}{4kT}\right) \right]}{\left(\frac{hw_0}{4kT}\right)} \dots\dots\dots(2.39)$$

The above Eq.(2.39) shows a decrease of activation energy with decrease of temperature.

2.4.4 Triberis and Friedman's Model:

Triberis and Friedman [38] and Triberis [39] have studied dc hopping conductivity in disordered systems at low and high temperatures using percolation considerations. In this case, the electronic transport is described as a single phonon-induced tunneling of electrons between localized states which are randomly distributed in energy and position. Considering correlation due to energy of common sites in a percolation cluster, the following expression for the conductivity has been obtained.

$$\sigma = \sigma_0 \exp\left[-\left(\frac{T_0}{T}\right)^{1/4}\right] \dots\dots\dots (2.40)$$

where T_0 is constant and has different forms at high and low temperatures. T_0 is given by

$$T_0 = \frac{C\alpha^3}{kN_0} \dots\dots\dots (2.41)$$

$$= 12.5 \alpha^3/kN_0 \quad \text{for high temperatures} \quad \dots\dots\dots (2.42)$$

$$= 17.8 \alpha^3/kN_0 \quad \text{for low temperatures} \quad \dots\dots\dots (2.43)$$

where N_0 (density of localized states) is assumed constant. Thus, the percolation

model of Triberis and Friedman predicts a $\left(\frac{1}{T}\right)^{1/4}$ dependence of the logarithmic conductivity in the high as well as low temperature region.

2.4.5 Killias Model:

Killias [40] has proposed a polaron model in which the variation of activation energy is considered due to the thermally activated hopping in a system which has a distribution of hopping distances. Assuming a Gaussian distribution for the hopping distances centered around a median value R_0 , Killias has obtained the following expression for the dc conductivity.

$$\sigma = A \exp \left[-\frac{W(R_0)}{kT} - \left(\frac{a}{2\beta kT} \right)^2 \right] \times \left[1 - \frac{1}{2} \operatorname{erfc} \left(\beta R_0 - \frac{a}{2\beta kT} \right) \right] \dots\dots\dots(2.44)$$

where A is a constant, $a=dW/dR$ and β^{-1} is proportional to the width of the Gaussian distribution. The above equation predicts a non linear variation of the dc conductivity which may be described most conveniently by a temperature dependent activation energy given by

$$W(T) = W_0 \left(1 - \frac{\theta_R}{T} \right) \dots\dots\dots(2.45)$$

where W_0 and θ_R are constant and θ_R is given by

$$\theta_R \approx \frac{a^2}{4\beta k W_0} \dots\dots\dots(2.46)$$

2.5 Models for AC conductivity:

In general, electrical characterization of the materials can be done by dc and ac measurement technique. Though the dc measurement technique is straight

forward, it cannot be implemented for ionic or mixed electronic-ionic systems because on application of dc field, the ionic material gets polarized. Due to which the ionic conductivity gradually ceases, giving only electronic conductivity. To overcome the above problem, ac technique is preferred over dc technique.

Frequency dependent conductivity behavior of ionically conducting glasses has been the focus for large number of studies [41-44] although very limited understanding of this multi-faceted problem has been achieved so far. While there are large number of theories, to explain the dispersion behavior of glasses, among them universal model for ac transport seems to have been successful. Jonscher [42] has proposed a universal model, which describes the dispersion behavior observed in ac conductivity.

According to *Jonscher's universal power law*, the variation of ac conductivity with frequency is given by $\sigma(\omega) = \sigma_0 + A\omega^n$. The log σ versus log frequency plot enables us to visualize the range of ionic phenomena from long range displacement to resonant vibration. It was evident from log-log plot of conductivity that at high frequencies $\sigma(\omega)$ follows an apparent power law, $\sigma(\omega) \propto \omega^n$, where n is power law exponent while at low frequencies, there is a gradual transition to frequency independent conductivity.

In *jump relaxation model*, Funke [45] has proposed that the dc plateau and the power law region should be considered as a single entity. Both these regions together represent '*successful*' and '*unsuccessful*' hopping of the mobile ions. According to this model, at very low frequencies ($\omega \rightarrow 0$), an ion can jump from one site to its neighboring vacant site successfully contributing to dc conductivity. At high frequency, the probability for the ion to go back again to its initial site

increases due to the short time periods available. This high probability for the correlated forward backward hopping at high frequencies together with the relaxation of the dynamic cage potential is responsible for the high frequency dispersion.

The relaxation process in glasses is generally non-Debye in nature. Kawamura et.al. [46] have explained the origin of non exponential (non-Debye) behavior in phosphate glasses by considering the effective random potential acting on a mobile charge. Different approaches have been taken by Jonscher [47] and Ngai [48] accounting for the non-exponential behavior by considering many body effects and by the fractional exponential relaxation formalism in association with coupling theory respectively. The many body interaction among mobile ions is significant in high ion conducting glasses. The *universal theory* by Jonscher [41, 42], *coupling theory* [49], *cluster relaxation theory* [50], *diffusion controlled relaxation model* [51, 52] and *Debye-Falkenhagen-type theory* [53] supports this view point.

AC Conductivity over wide ranges of temperature and frequency have shown that a single power law is inadequate to describe the dispersion of conductivities in many cases, therefore, in that case a double power law of the form $\sigma(\omega)=\sigma_0+A\omega^{n1}+B\omega^{n2}$ describes the ac conductivity better than a single power law. The behavior of the first region, in the double power law equation can be described by the *Diffusion Controlled Relaxation* model (DCR model) of Elliot [51, 52].

The electric field relaxation due to the motion of ions is first described by

Kohlrausch William Watt exponent [54, 55, 56] $\phi(t) = \exp\left[-\left(\frac{t}{\tau_\sigma}\right)^\beta\right]$, where τ_σ

and β are the parameters of stretched exponential function and are respectively the conductivity relaxation time and the Kohlrausch exponent. The values of β varies from 1 to 0. The smaller is the value of β , the larger is the deviation of the relaxation with respect to a Debye type relaxation. Ngai [49] has proposed that a correlation exists between n and β , namely $n = 1 - \beta$. Several other attempts have also been made to correlate β with a large number of parameters like Structural Unpinning Number (SUN) [57] and intercationic distance [58]. The β parameter has been interpreted either as representatives of a distribution of relaxation times [59, 60] or as characteristic of cooperative motions between charge carriers [61, 48]. The concept of the cooperative motions in a glass is issued from the 'universal' behavior discussed by Jonscher [47]. It means that jump of a mobile ion in a glass may not be treated as an isolated event i.e., when the ion jumps from one equilibrium position to another it causes a time dependent movement of other charge carriers in the surroundings, which leads to additional relaxation of the applied field [62]. So it results the smaller value of β to a more extended co-operation between the charge carriers [62].

2.6 Theoretical details of different characterization techniques:

Different experimental techniques have been used to characterize the glassy samples which are discussed briefly in the sub-sections below.

2.6.1 X-Ray Diffraction:

X-ray diffraction is based on the constructive interference of monochromatic x-rays from a crystalline sample. These x-rays are generated by a cathode ray tube, filtered to produce monochromatic radiation, collimated to concentrate and directed toward the sample. The interaction of the incident rays with the sample produces constructive interference (and a diffracted ray) when conditions satisfy Bragg's law [Fig.2.2] ($n\lambda=2d \sin \theta$) where λ is the wavelength in Å, d is the interatomic spacing in angstroms, θ is the diffraction angle in degrees and n is an integer representing the order of the diffraction peak. This law relates the wavelength of electromagnetic radiation to the diffraction angle and the lattice

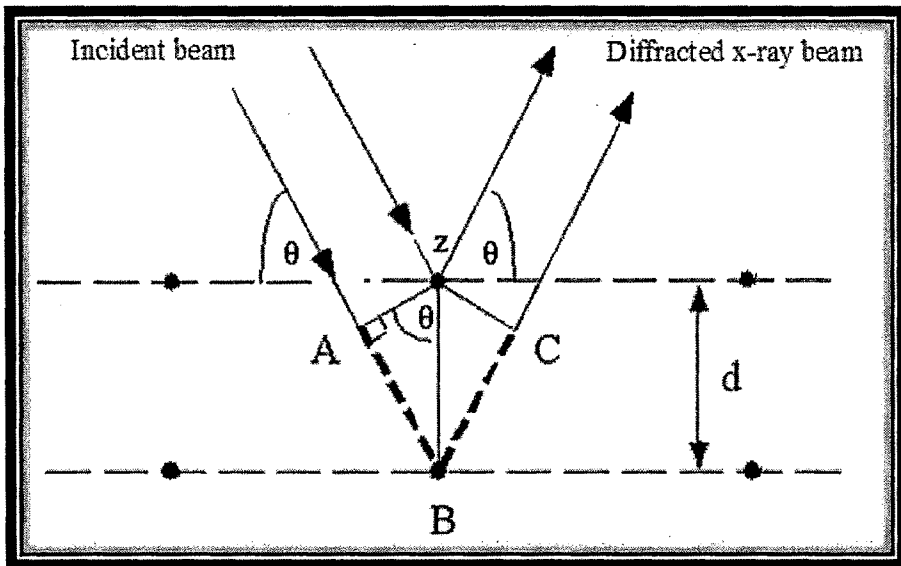


Fig.2.2. Schematic representation of diffraction X-rays by crystal.

spacing in a crystalline sample. These diffracted x-rays are then detected, processed and counted by scanning the sample through a range of 2θ angles. All possible diffraction directions of the lattice should be attained due to the random orientation of the powdered material. Conversion of the diffraction peaks to d-spacing allows identification of the mineral because each mineral has a set of unique d-spacings.

X-rays are electromagnetic radiation with typical photon energies in the range of 100 eV-100 KeV. For diffraction applications, only short wavelength x-rays (hard x-rays) in the range of a few angstroms to 0.1 Å (1 KeV-120 KeV) are used. Diffraction is most effective when the wavelength of the incident radiation is comparable to the size of the diffracting object. Diffraction occurs as waves interact with a regular structure whose repeat distance is about the same as wavelength. Diffracted waves from different atoms can interfere with each other and the resultant intensity distribution is strongly modulated by this interaction. In crystals, the diffracted waves will consist of sharp interference maxima (peaks) with the same symmetry as in the distribution of atoms while for amorphous sample, diffraction pattern shows few diffused halos instead of sharp peaks.

2.6.2 Differential Scanning Calorimetry:

One of the techniques used for characterization is the thermal analysis technique, which is based on the relationship between temperature and some property of a system such as mass, heat of reaction or volume. Le Chatelier [63] was the father of thermal analysis. After that other investigators [64-67] have studied the thermal changes in a substance during the heat treatment. Thermogravimetry (TG), Differential Thermal Analysis (DTA), Differential Scanning Calorimetry (DSC),

Enthalpimetric Method are the different methods used for thermal investigations [68, 69].

Differential Scanning Calorimetry is a thermoanalytical technique in which the difference in the amount of heat required to increase the temperature of the sample and reference are measured as a function of temperature. Both the sample and reference are maintained at nearly the same temperature throughout the experiment. Generally, the temperature program for a DSC analysis is designed such that the sample holder temperature increases linearly as a function of time. The reference sample should have a well defined heat capacity over the range of temperatures to be scanned. Fig. 2.3 shows the cross sectional diagram of DSC cell. In the cell, a metallic disc (made of constantan alloy) is the primary means of heat transfer to and from the sample and the reference. The sample contained in a metal pan and the reference (an empty pan) sit on raised platforms formed in the constantan disc. As heat transferred through the disc, the differential heat flowing to the sample and reference is measured by thermocouples formed by the junction of the disc and chromel wafers which cover the underside of the platforms. These thermocouples are connected in series and measure the differential heat flow using the thermal equivalent of ohms written as:

$$\frac{dQ}{dt} = \frac{\Delta T}{R_D} \dots\dots\dots(2.47)$$

where $\frac{dQ}{dt}$ is heat flow, ΔT is the temperature difference between reference and sample, R_D is the thermal resistance of the disc. The result of a DSC experiment is a curve of heat flux versus temperature as observed in Fig.2.4. In the DSC plot, exothermic peak is due to the evolution of heat from the sample which raises the

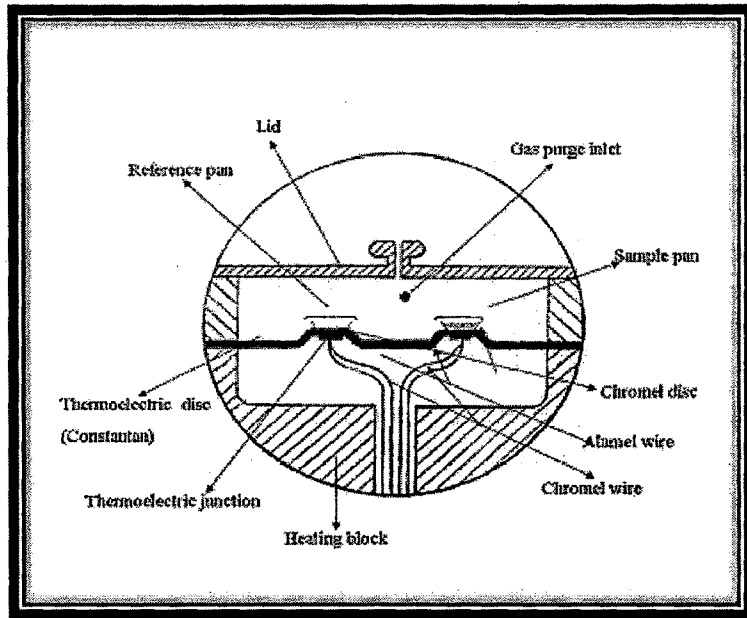


Fig.2.3. Crosssectional diagram of DSC heat flux.

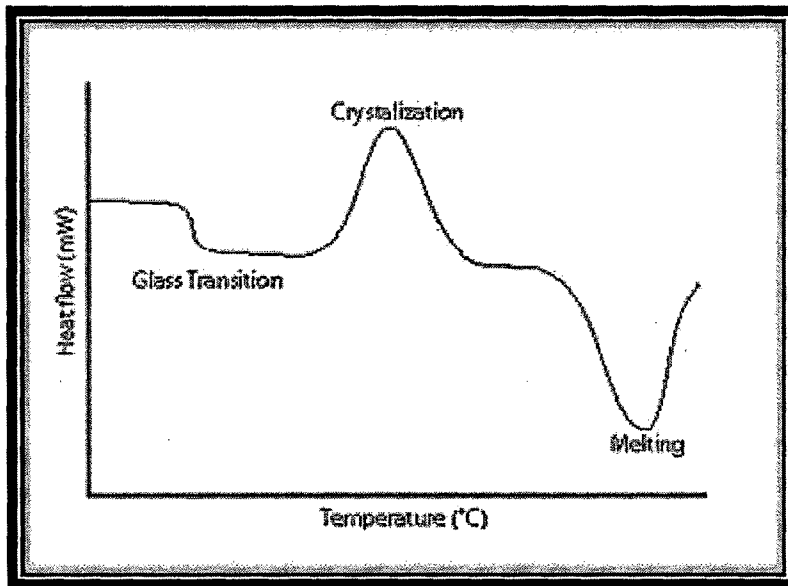


Fig.2.4. A schematic DSC curve demonstrating the appearance of several common features.

temperature temporarily above that of the reference material; whereas, endothermic peak is just due to the reverse type of process.

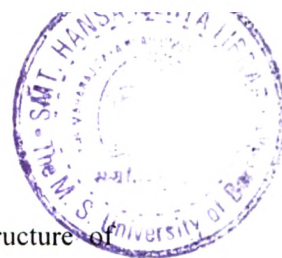
The main application of DSC is in studying phase transitions, such as melting, glass transitions and crystallization. These transitions involve energy changes or heat capacity changes that can be detected by DSC with great sensitivity.

Detection of Phase Transition:

The basic principle underlying this technique is that, when the sample undergoes a physical transformation such as phase transitions, more or less heat will need to flow through it than the reference, to maintain both at the same temperature. Flow of less or more heat through the sample, depends on whether the process is exothermic or endothermic. For example, as a solid sample melts to a liquid it will require more heat flowing to the sample to increase its temperature at the same rate as the reference. This is due to the absorption of heat by the sample as it undergoes the endothermic phase transition from solid to liquid. Likewise, as the sample undergoes exothermic processes (such as crystallization), less heat is required to raise the sample temperature. By observing the difference in heat flow between the sample and the reference, differential scanning calorimeters are able to measure the amount of heat absorbed or released during such transitions. DSC may also be used to observe more subtle phase changes, such as glass transitions. DSC is widely used in industrial settings as a quality control instrument due to its applicability in evaluating sample purity and for studying polymer curing [70-72].

2.6.2 Fourier Transform Infrared Spectroscopy:

IR Spectroscopy is a fundamental technique for chemical identification of a



functional group, which provides a useful information regarding structure of molecules. It involves the twisting, bending, rotating and vibrational motions of atoms in a molecule. Upon interacting with IR radiation, portions of the incident radiation are absorbed at particular wavelengths. The multiplicity of vibrations occurring simultaneously produces a highly complex absorption spectrum, which is unique characteristic of the functional groups comprising the molecule and of the overall configuration of the atoms as well.

Absorption in the infrared region results in changes in vibrational and rotational status of the molecules. The absorption frequency depends on the vibrational frequency of the molecules, whereas the absorption intensity depends on how effectively the infrared photon energy can be transferred to the molecule and this depends on the change in the dipole moment that occurs as a result of molecular vibration. As a consequence, a molecule will absorb infrared light only if the absorption causes a change in the dipole moment and known as "*IR active molecule*". Thus, all those compounds which are IR active can be analyzed by their characteristic infrared absorption.

Fig.2.5 shows the optical diagram of the Fourier transform Infrared spectrometer. From the IR source light travels to the beam splitter, 50% of the light is reflected to the fixed mirror and 50% is transmitted to the movable mirror. Light travels to each of the mirrors and recombines at the beam splitter before passing through the sample and to the detector. As the light intensity of the recombined beam is recorded at the detector, the movable mirror travels towards the beam splitter, producing an interferogram. As the movable mirror travels, different frequencies are reflected in different ways. The summation of constructive and destructive

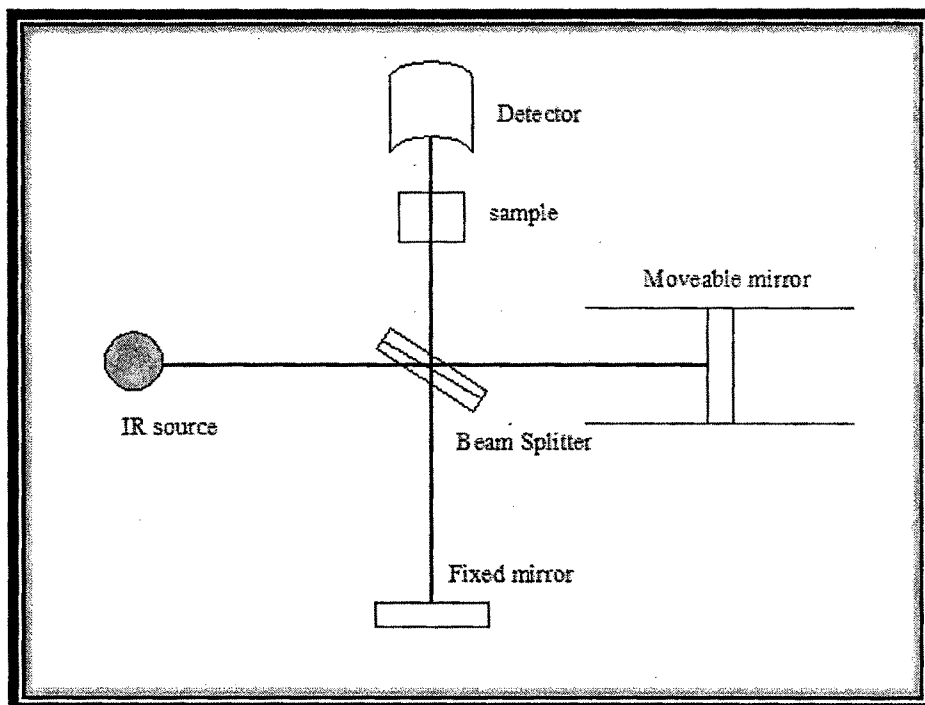


Fig.2.5. The optical diagram of a Fourier transform Infrared Spectrometer.

interference over time makes an interferogram, from which a Fourier transform is used to calculate a spectrum.

FTIR provides the following information →

- ❖ It can identify unknown materials.
- ❖ It can determine the quality or consistency of a sample.
- ❖ It can determine the amount of components in a mixture.

2.6.3.1 Requirements for absorption of IR:

A natural vibrational mode within a molecule will absorb IR radiation, if the following conditions are fulfilled.

1) Those molecules will absorb IR radiation in which the natural frequency of vibration of the molecule is the same as the frequency of the incident radiation. The IR radiation, that is absorbed, causes the molecule to vibrate at increased amplitude (Resonance).

2) Those molecules can absorb IR radiation in which absorption produces some changes in the electric dipole of the molecules. Such molecules are known as IR active materials. The dipole moment is determined by the positions of the centers of gravity of the positive and negative electrical charges. When a molecule having electric dipole is kept in the electric field, it exerts a force on the electric charges in the molecules, which gives rise to decrease or increase of a separation. Change in the electric field of IR radiation causes a change in polarity periodically, it means that the spacing between the charged atoms of the molecule also changes periodically and vibration of these charged atoms causes the absorption of IR radiation. In symmetrical stretching vibration, the centers of gravity of the charges coincide in every vibrational position, no dipole moment is created and the absorption characteristic of this mode is not observed in IR. Such vibrations are said to be IR inactive. However, in unsymmetrical stretching vibration, a dipole moment is produced and the vibration is IR active and is observed in IR spectrum.

2.6.3.2 Theory of IR absorption spectroscopy:

The position of atoms in a molecule is not fixed; they are subjected to a number of different vibrations and rotations. Two atoms are joined by a covalent bond which may undergo stretching vibrations. The atoms can undergo a variety of stretching and bending vibrations. Energy of a vibration depends on (1) the mass of the atom

present in a molecule, (2) strength of a bond and (3) the arrangement of various atoms in a molecule.

The position of IR band is described in terms of wavelength λ (usually measured in microns, μ) or wave number, $\bar{\nu}$. Both these units are related to each other by the relation

$$\bar{\nu}(\text{in } cm^{-1}) = \frac{10^4}{\lambda} (\text{in } \mu) \dots\dots\dots(2.48)$$

The positions of absorption bands, as determined from the mechanical theory of harmonic oscillators, are given by [73]

$$\bar{\nu} (\text{in } cm^{-1}) = \frac{1}{2\pi c} \sqrt{\frac{k(m_1 + m_2)}{m_1 m_2}} \dots\dots\dots(2.49)$$

where m_1 and m_2 are the masses of two adjacent atoms in a molecule and k is the restoring force per unit displacement and can be expressed as

$$k = aN \left(\frac{\chi_1 \chi_2}{d^2} \right)^{3/4} + b \dots\dots\dots(2.50)$$

where N is the band order (i.e., effective number of covalent or ionic bands), χ_1 and χ_2 are the electro negativities of the atoms, d is the internuclear distance in angstroms and $a(=1.67)$ and $b(=0.30)$ are constants. From the above relations, it is clear that the bond length can be a good guide to the direction of a shift of band resulting from a change in chemical group- the greater the length, the lower the frequency. Bending modes usually produce lower frequency absorption bands than fundamental stretching modes.

2.6.3.3 Stretching vibrations:

It arises due to stretching and contracting of bond without producing any change in the bond angles, which are of two types.

1) Symmetric stretching:

If the movement of atoms with respect to a particular atom in a molecule is in the same direction, it is called symmetrical stretching vibrations as shown in Fig. 2.6.

2) Asymmetric stretching:

If one atom approaches the central atom whereas the other approaches away from it in a triatomic system, it gives unequal movement of the outer atom with respect to central one, as shown in Fig. 2.7. Because of this, the change in electric dipole takes place. Therefore, asymmetric stretching gives it vibrational frequency at higher wavenumber than for symmetric system.

2.6.3.4 Bending vibrations:

It gives rise to deformation of bond angle but there is no change in bond lengths.

In molecules, most of the bond angles are found to be in two categories.

- 1) Linear or 180° bond angle.
- 2) Bond angle in a neighborhood of 120° to 110°.

In triatomic molecules, the two atoms are the same and are bound to the middle atom by two equal bonds with two different frequencies symmetric or asymmetric.

$$\nu_{sym} (cm^{-1}) \approx \left(\frac{1}{2\pi c} \right) \left[k \left\{ \frac{1}{m_{end}} + \frac{(1 + \cos \alpha)}{m_{mid}} \right\} \right]^{1/2} \dots\dots\dots(2.51)$$

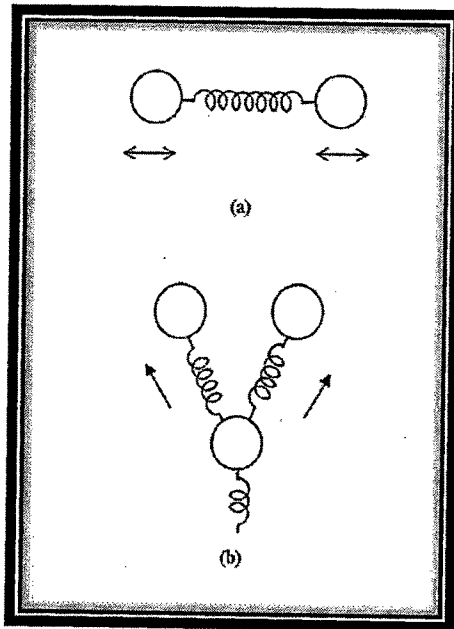


Fig.2.6: Symmetric Stretching Vibrations: (a) Diatomic Molecule (b) Triatomic Molecule.

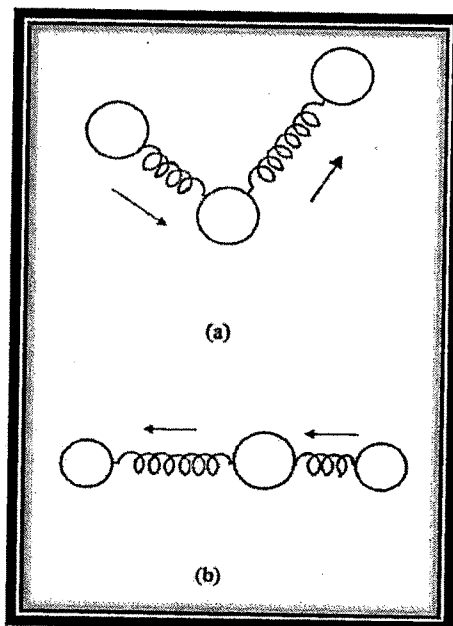


Fig.2.7: Asymmetric Stretching Vibrations: (a) and (b) Triatomic Molecule.

$$\nu_{\text{asym}}(\text{cm}^{-1}) \approx \left(\frac{1}{2\pi c} \right) \left[k \left\{ \frac{1}{m_{\text{end}}} + \frac{(1 - \cos \alpha)}{m_{\text{mid}}} \right\} \right]^{1/2} \dots\dots\dots(2.52)$$

where α is a bond angle, ν is a frequency in cm^{-1} , k is the force constant in dyne/cm, m_{end} and m_{mid} are the masses of one end and middle atom respectively.

The above Eqn. 2.51 and 2.52 can also be written as.

$$\nu_{\text{sym}}(\text{cm}^{-1}) \approx \left(\frac{1}{2\pi c} \right) \left[k \left\{ \frac{1}{M_{\text{end}}} + \frac{(1 + \cos \alpha)}{M_{\text{mid}}} \right\} \right]^{1/2} \dots\dots\dots(2.53)$$

$$\nu_{\text{asym}}(\text{cm}^{-1}) \approx \left(\frac{1}{2\pi c} \right) \left[k \left\{ \frac{1}{M_{\text{end}}} + \frac{(1 - \cos \alpha)}{M_{\text{mid}}} \right\} \right]^{1/2} \dots\dots\dots(2.54)$$

where M_{end} and M_{mid} are the atomic weights of end atom and middle atoms.

A number of boro-vanadate, barium vanadate and barium boro-vanadate glasses were studied [74-76]. In these glasses the vibrational frequency of a bond V-O-V type can be given by [74] Eqn. 2.53 and 2.54, where $M_{\text{end}} = M_{\text{V}}$ and $M_{\text{mid}} = M_{\text{O}}$ are the atomic weights of vanadium and oxygen atoms respectively. α is a bond angle (always greater than 90°) between V-O-V bonds [Fig. 2.8 & 2.9]. In glasses, the bonds are generally broader and overlapping than those observed in the crystalline materials. This is because of the lack of long range order in glasses and is similar to the broadening of the spectra observed in other techniques (e.g., X-ray diffraction, Mossbauer spectra) [77-80].

Bending vibrations are classified into four types, in Fig. 2.8 (a, b) and Fig. 2.9 (a, b).

(1) Scissoring Bending:

In this type of bond vibrations, the two atoms approach each other in the same

plane as shown in Fig. 2.8 (a).

(1) Rocking Bending:

In this type of bond vibrations, the movements of atom occur in the same direction and also in the same plane as shown in Fig.2.8 (b).

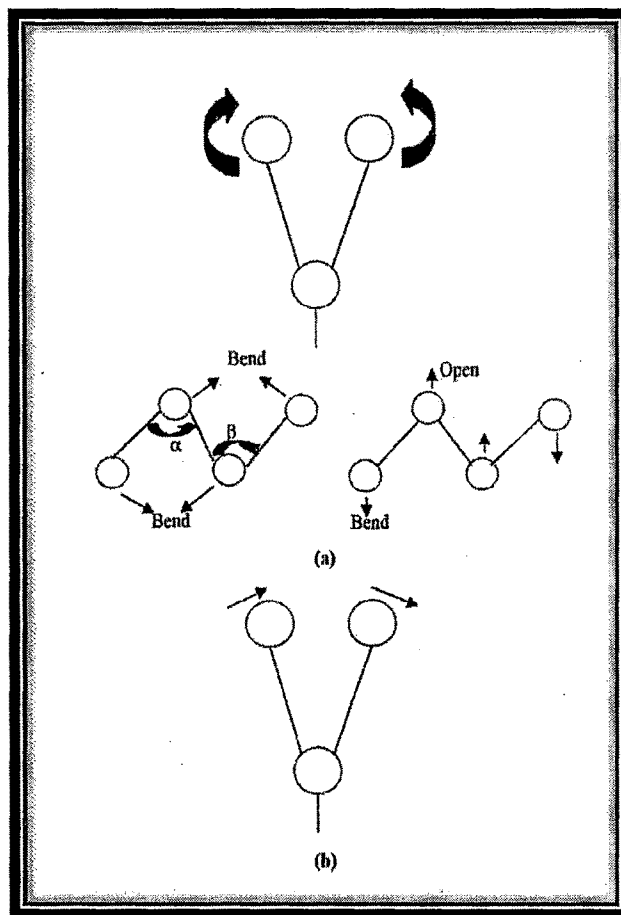


**Fig.2.8: (a) Scissoring Bending (In plane bending with lower frequency of vibration).
(b) Rocking Bending (In plane bending with lower frequency of vibration).**

(2) Wagging Bending:

In this type of bond vibrations, the two atoms move up and down below the plane with respect to the central atom as shown in Fig.2.9 (a).

(4) Twisting Bending:

In this type of vibrations, one of the atoms moves up the plane and the other moves down the plane with respect to the central atom as shown in Fig.2.9 (b).

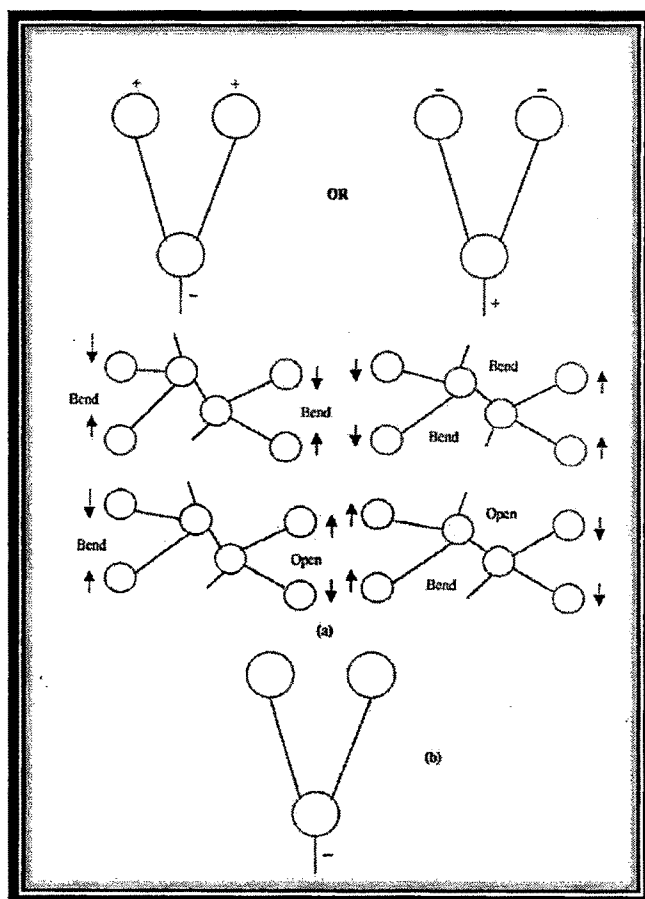


**Fig. 2.9: (a) Wagging Bending (Out of plane having high frequency of vibration).
(b) Twisting Bending (Out of plane bending with high frequency of vibration).**

Here (+ve) and (-ve) sign represents motion above and below the plane of the paper respectively. The energy required to stretch a spring is more than that needed to bend it so the stretching absorption of the bond will appear at higher frequencies than the bending absorption of a bond. Thus IR spectroscopy is widely used for molecular structural studies of various glasses.

Fourier transform infrared spectroscopy is preferred over dispersive or filter methods of infrared spectral analysis for several reasons:

- ❖ It is a non-destructive technique.
- ❖ It provides a precise measurement method which requires no external calibration.
- ❖ It can increase speed, collecting a scan every second.
- ❖ It can increase sensitivity – one second scans can be co-added together to ratio out random noise.
- ❖ It has greater optical throughput.
- ❖ It is mechanically simple with only one moving part.

2.7. Transport number measurement:

The transference number of a glass system signifies the contribution of ionic conductivity to the total conductivity. Therefore, it is one of the key factors to be considered while choosing the system as an electrolyte (in super ionic system) or to be used as a cathode material (in mixed conducting system) for battery application. Normally, the transport number measurement can be carried out through different methods namely, Tubandt's method [81], Hebb-Wagner's polarization method [82] and electrochemical (EMF) method [83]. The electronic

contribution to the total conductivity can be obtained from Wagner polarization technique, whereas the other techniques brief about ionic nature of the conducting species.

The transport number of a moving charged particle is defined as the ratio of the conductivity due to itself and the total conductivity. There are many methods to ensure the transference number. In Wagner polarization technique [84-86], the sample is placed between two electrodes, one blocking and the other non-blocking for the mobile ionic species. Current versus time is monitored for a fixed applied dc potential. The initial total current decreases with time due to the depletion of ionic species in the samples and becomes constant in the fully depleted situation. At this stage, the residual current is only electronic current. The electronic transference number t_e and the ionic transference number t_i respectively are given by

$$t_e = \frac{\sigma_e}{\sigma_T} = \frac{i_e}{i_T} \dots\dots\dots(2.55)$$

and $t_i = 1 - t_e \dots\dots\dots(2.56)$

where σ_e and σ_T are the electronic conductivity and total conductivity respectively while i_e is the electronic current and i_T is the total current.

1) **EMF method:**

Transference number can also be measured by EMF method [84, 87]. In this method the ionic conductor is placed between a pair of electrodes of different chemical potentials μ_1 and μ_2 . The potential difference (emf) developed across the electrodes is given by [83]

$$E_{obs} = \frac{-1}{|Z|F} \int_{\mu_1}^{\mu_2} t_i d\mu = \frac{t_i(\mu_1 - \mu_2)}{|Z|F} = \frac{t_i \Delta G}{F|Z|} \dots\dots\dots(2.57)$$

where t_i is the ionic transport number, μ_1 and μ_2 are chemical potential of the electrodes, ΔG is the change in free energy involved for a given pair of electrodes, $|Z|$ is the valence of mobile ion and F is the Faraday's constant. For an ideal electrolyte with $t_i = 1$, the emf generated is given by

$$E_{theo} = \frac{\Delta G}{F|Z|} \dots\dots\dots(2.58)$$

From the above relations, $E_{obs} = t_i E_{theo}$. Thus the transport number of the mobile ion can be calculated from the ratio of observed emf (E_{obs}) to the theoretical value of emf (E_{theo}) for a given pair of electrodes.

References:

- [1] N. F. Mott, *J. Non-Cryst. Solids*, 1 (1968) 1.
- [2] I. G. Austin, N. F. Mott, *Adv. Phys.*, 18 (1969) 41.
- [3] M. Sayer, A. Mansingh, *Phys. Rev. B* 6 (1972) 4629.
- [4] C. H. Chung, J. D. Mackenzie, *J. Non-Cryst. Solids* 42 (1980) 151.
- [5] A. E. Owen, *J. Non-Cryst. Solids*, 25 (1977) 370.
- [6] A. Ghosh, *J. Phys. Condens. Matter* 1 (1989) 7819.
- [7] A. Ghosh, *Philos. Mag. B* 61 (1990) 87.
- [8] P. W. Anderson, *Phys. Rev.* 109 (1958) 1492.
- [9] A. Miller, E. Abraham, *Phys. Rev.* 120 (1969) 745.
- [10] L. Murawski, C. H. Chung, J. D. Mackenzie, *J. Non-Cryst. Solids*, 32 (1979) 91-104.
- [11] T. Holstein, *Ann. Phys.* 8 (1959) 325; *ibid* 8 (1959) 343.
- [12] A. P. Schmid, *J. Appl. Phys.*, 39, 7 (1968) 3140
- [13] J. Frenkel; *Z. Physik* 35 (1926) 657.
- [14] J. C. Bazan, J. A. Duffy, M. D. Ingram, M. R. Mallance, *Solid State Ionics* 86-88 (1996) 497.
- [15] G. Jayasinghe, M. Dissanayake, M. Careem, J. L. Souquet, *Solid State Ionics* 93 (1996) 291.
- [16] M. Wasiucione, J. Garbarczyk, B. Wnetrzewski, P. Machowski, W. Jakubowski, *Solid State Ionics* 92 (1996) 155.
- [17] J. Garbarczyk, M. Wasiucione, B. Wnetrzewski, W. Jakubowski, *Phys. Status Solidi (a)* 156 (1996) 441.
- [18] K. Krasowski, J. Garbarczyk, *Phys. Status Solidi (a)* 158 (1996) K13.

- [19] P. Sathya, Sainatah Prasad, S. Radhakrishna, *J. Mater. Sci.* 23 (1988) 4492.
- [20] N. F. Mott, *Philos. Mag.* 19 (1969) 835.
- [21] C. Cramer, K. Funke, B. Roling, T. Saatkamp, D. Wilmer, M. D. Ingram, A. Pradel, M. Ribes, G. Taillades, *Solid State Ionics* 86-88 (1996) 481.
- [22] I. G. Austin, *J. Non-Cryst. Solids* 2 (1970) 474.
- [23] N. F. Mott, E. A. Davis, *Electronic processes in Non-Cryst. Solids* 2nd ed., Clarendon Oxford, 1979.
- [24] H. Mori, K. Gotoh, H. Sakata, *J. Non-Cryst. Solids*, 18 3 (1995) 122.
- [25] V. Ambegaokar, S. Cochran, J. Kurkijarvi, *Phys. Rev. B* 8 (1973) 3682.
- [26] A. Al-Shahrani, M. M. El-Desoky, *J. Mat. Sci: Materials In Electronics* 17 (2006) 43-49.
- [27] T. Holstein, L. Friedman, *Ann. Phys.* 21 (1963) 494.
- [28] T. Holstein, D. Emin, *Ann. Phys.* 53 (1969) 439.
- [29] V. K. Dhawan and A. Mansingh, *J. Non-Cryst. Solids* 51 (1982) 87-103.
- [30] M. Sayer, A. mansingh, *J. Non-Cryst. Solids*, 58 (1983) 91.
- [31] M. M. Moawad, H. Jain, R. El-Mallawany, *J. Phys. Chem. Solids* 70 (2009) 224-233.
- [32] S. Hazra, A. Ghosh, *J. Chem. Phys.* 103 (1995) 6270-6274.
- [33] H. Mori, H. Matsuno, H. Sakata, *J. Non-Cryst. Solids* 276 (2000) 78-94.
- [34] S. Hazra, S. Mandal, A. Ghosh, *J. Chem. Phys.* 104 (1996) 10041-10045.
- [35] H. Hirashima, D. Arai, T. Yoshida, *J. Am. Ceram. Soc.* 68, 9 (1985) 486-489.
- [36] A. Ghosh, B. K. Chowdari, *J. Non-Cryst. Solids* 83 (1986) 151.
- [37] J. Schnakenberg, *Phys. Status Solidi* 28 (1968) 623.

- [38] G. P. Triberis, L. R. Friedman, *J. Phys. C* 18 (1985) 2281.
- [39] G. P. Triberis, *J. Non-Cryst. Solids* 74 (1985) 1.
- [40] H. R. Killias, *Phys. Lett.* 20 (1966) 5.
- [41] A. K. Jonscher, *J. Phys. C: Solid State Phys.* 6 (1973) 1235.
- [42] A. K. Jonscher, *J. Mat. Sci.* 16 (1981) 2037.
- [43] K. Funke, *Z. Phys. Chem. (NF)* 154 (1987) 251.
- [44] H. Jain, J. N. Mundy, *J. Non-Cryst. Solids* 91 (1987) 315.
- [45] K. Funke, *Solid State Ionics* 18-19 (1986) 183; *Prog. Solid State Chem.* 22 (1992) 111.
- [46] J. Kawamura, M. Shimoji, *J. Non-Cryst. Solids* 79 (1986) 367.
- [47] A. K. Jonscher, *Nature* 267 (1977) 673.
- [48] K. L. Ngai, H. Jain, *Solid State Ionics* 18/19 (1986) 362.
- [49] K. L. Ngai, *Solid State Physics* 9 (1979) 127; 9 (1980) 141.
- [50] L. A. Dissado, R. M. Hill, *Solid State Ionics* 22 (1987) 331.
- [51] S. R. Elliott, *Solid State Ionics*, 27 (1988) 131.
- [52] S. R. Elliott, A. P. Owens, *Phil. Mag. B* 60 (1989) 777.
- [53] M. Tomozawa, in: *Treatise on Material Science*, ed. H. Hannay, (Academic Press, New-York, 1977) 283.
- [54] G. Williams, D. C. Watts, *Trans. Faraday Soc.* 23 (1970) 625.
- [55] K. L. Ngai, S. W. Martin, *Phys. Rev. B* 40 (1989) 10550.
- [56] F. S. Howell, R. A. Bose, P. B. Macedo, C. T. Moynihan, *J. Phys. Chem.* 78 (1974) 639.
- [57] M. C. R. Shastry, K. J. Rao, *Solid State Ionics* 44 (1991) 187.
- [58] J. M. Reau, S. Rossignol, B. Tanguy, J. M. Rojo, P. Herrero, R. M. Rojas, J. Sanz, *Solid State Ionics* 74 (1994) 65.

- [59] R. J. Grant, M. D. Ingram, L. D. S. Turner, C. A. Vincent, *J. Phys. Chem.* 82
26 (1978) 2838.
- [60] C. T. Moynihan, L. P. Boesch and N. L. Laberge, *Phys. Chem. Glasses* 14
(1973) 122.
- [61] K. L. Ngai, J. N. Mundy, H. Jain, G. Baver-Jollenbeck and O. Kanert, *Phys.*
Rev. B 39 (1989) 169.
- [62] H. Jain, *J. Non-Cryst. Solids* 131/133 (1991) 961.
- [63] Le Chatelier H., *Bull. Soc. Franc. Mineral* 10, 203 (1987).
- [64] Ashley H. F. *Ind. Eng. Chem.* 3, 91 (1911).
- [65] Rieke R., *Sprechsaal*, 44, 637-840 (1911).
- [66] Wallach H., *Compt. Rend*, 157, 48 (1913).
- [67] Meeler J. W. and A. D. Holdcraft, *Trans. Brit. Cerm. Soc.* 10, 94 (1910-
1911).
- [68] W. W. Wendlandt "Thermal methods of analysis", 2nd ed. P. 172, Wiley,
New York, 1974.
- [69] T. Meisel and K. Seybold, *Crit. Rev. and Chem.* 12 (1981) 267.
- [70] Dean, John A. "The analytical chemistry Handbook", New York, Mc Graw
Hill, Inc. 1995, pp. 15.1—15.5.
- [71] Pungor, erno. *A Practical guide to Instrumental analysis*, Boca Ranton,
Florida, 1995, pp. 181-191.
- [72] Skoog, Douglas A., F. James Holler and Timothy Nieman, *principles of*
Instrumental analysis, Fifth edition, New York 1998, 905-908.
- [73] H. H. Wilard, L. L. Merritt, Jr. J. A. Dean, 'Instrumental methods of
analysis', *Affiliated East West Press Pvt. Ltd.*, New Delhi, Fourth Edition,
1965, p. 124.

- [74] P. Gray, L. C. Klein, *J. Non-Cryst. Solids* 68 (1984) 75.
- [75] A. M. Sanad, I. F. Kashif, A. A. Sharkawy, A. A. El-Saghier, *J. Mater. Sci.* 21 (1986) 3483.
- [76] R. Nadjd-Sheibani, C. A. Hogarth, *J. Mater. Sci.* 26 (1991) 429.
- [77] C. R. Kurjjain, E. A. Sigety, *Phys. Chem. Glasses* 9 (1968) 73.
- [78] C. R. Kurjjain, *J. Non-Cryst. Solids* 3 (1970) 157.
- [79] T. K. bansal, R. G. Mendiratta, *Phys. Chem. Glasses*, Vol 28, No. 6 (1987) 235.
- [80] T. Nishida, Y. Takashima, *J. Non-Cryst. Solids* 94 (1987) 229.
- [81] C. Tubandt, *Z. Anorg. Allg. Chem.* 115 (1921) 105-126.
- [82] J. B. Wagner, C. Wagner, *J. Chem. Phys.* 26 (1957) 1597-1601.
- [83] K. Kiukkola, C. Wagner, *J. Electrochem. Soc.* 104 (1957) 379-387.
- [84] S. Chandra, *Super ionic Solids-Principles and Applications*, North-Holland, Amsterdam, 1981.
- [85] J. Schoonman, F. G. Dijkman, *J. Solid State Chem.* 5 (1972) 111-117.
- [86] A. V. Joshi, J. B. Wagner, *J. Phys. Chem. Solids* 33 (1972) 205-210.
- [87] A. Dalvi, K. Shahi, *Solid State Ionics* 159 (2003) 369-379.